Non-invasive feedback stabilization of smooth and non-smooth nonlinear systems

G. Abeloos [1], **C. Collette** [1,2], **G. Kerschen** [1]
[1] University of Liège, Department of Aerospace and Mechanical Engineering,
Place du 20-Août, 7, B-4000 Liège, Belgium

[2] Université Libre de Bruxelles, Bio, Electro and Mechanical Systems Department,
Avenue F.D. Roosevelt, 50, B-1050 Brussels, Belgium

Abstract
Unstable periodic orbits of nonlinear structures can be stabilized through differential control of the displacement. However, nonlinearities in the system generate non-fundamental harmonics that are fed back into the excitation signal, affecting the structure's response and making the controller invasive. Adaptive filters are used to perform an online estimation of the Fourier coefficients of the displacement signal in order to cancel the invasiveness. The performance of the method is discussed for simulated experiments possessing smooth and non-smooth nonlinearities.

1 Introduction

The dynamics of a nonlinear system can be characterized through the identification of the periodic orbits it follows when responding to a monoharmonic excitation. While it can be straightforward to identify stable periodic orbits, there exist branches of unstable orbits that cannot be directly observed experimentally. One solution is to use non-invasive feedback control such that the asymptotically vanishing action of the controller modifies the system's dynamics until it is stable [1]. Because the control is non-invasive, the periodic orbits of the controlled system are identical to those of the uncontrolled one.

Stabilizing the nonlinear system allows the identification of whole branches of periodic orbits [2] and of bifurcations between such branches [3] by performing an experimental control-based continuation similar to what is done numerically. This method was able to characterize systems such as a vertically forced pendulum [4] or a nonlinear energy harvester [5]. The necessity to use expensive continuation algorithms (e.g. the pseudo-arclength method) can be avoided by choosing the continuation parameter to be the target amplitude rather than a physical parameter [6], rendering control-based continuation faster and computationally lighter. The method can be used to identify backbones of nonlinear systems [7], estimate the stability of the orbits being identified [8], track bifurcations [9], or characterize multi-degree-of-freedom systems with harmonically coupled modes [10].

In its state-of-the-art formulation, control-based continuation achieves non-invasiveness through an iterative procedure [6]. During each of the corrective iterations, the system must first reach steady-state before any measurement can be made. This work introduces a method to achieve non-invasiveness in an online manner by using adaptive filtering, meaning that the control is directly non-invasive when the system reaches steady-state. Section 2 illustrates how feedback control stabilizes the unstable periodic orbits of two virtual nonlinear systems, one possessing a smooth nonlinear stiffness and the other a non-smooth one. Section 3 shows how the stabilization is in general invasive and under which conditions it is not. Adaptive filters are introduced in Section 4 to cancel the invasiveness online. A parameter study is made in Section 5 to assess the performance of the method on the two systems possessing nonlinear stiffness and on a third system that does not exhibit unstable orbits, possessing a non-smooth discontinuous friction nonlinearity. This work is finally concluded in Section 6.

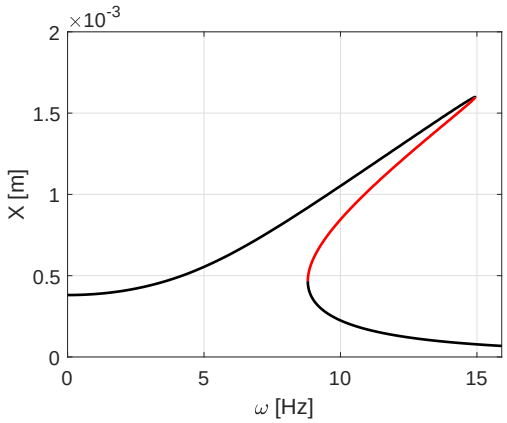

(a) Cubic system (cubic stiffness)

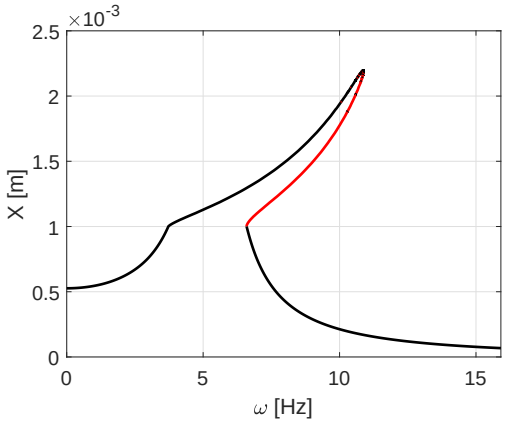

(b) Piecewise linear system (piecewise linear stiffness)

Figure 1: Frequency Response Curves of the nonlinear systems for excitation amplitude $F = 0.03$ N; stable orbits in black and unstable orbits in red

2 Feedback stabilization

Nonlinear systems respond in general to the following equation of motion defining the relation between the displacement x and the excitation f:

$$M\ddot{x}(t) + C\dot{x}(t) + Kx(t) + f_{\text{NL}}(x, \dot{x}, t) = f(t) \tag{1}$$

with the linear mass, damping, and stiffness matrices M, C, and K respectively. The internal nonlinear force f_{NL} generally depends on x and/or $\dot{x}$ corresponding to nonlinear stiffness and damping respectively. This paper considers single degree-of-freedom virtual experiments having identical linear coefficients shown in Table 1. One structure has a cubic stiffness:

$$f_{\text{NL},1}(x, \dot{x}, t) = 2 \cdot 10^8 \, x^3 \tag{2}$$

and is called the cubic system. Another has a piecewise linear stiffness:

$$f_{\text{NL},2}(x, \dot{x}, t) = \begin{cases} 400x + 0.4 & \text{for } x < -1 \text{ mm} \\ 0 & \text{for } -1 \text{ mm} \leq x < 1 \text{ mm} \\ 400x - 0.4 & \text{for } x \geq 1 \text{ mm}, \end{cases} \tag{3}$$

called the piecewise linear system.

Table 1: Linear parameters of the virtual experiments

M [kg]	C [Ns/m]	K [N/m]
0.05	0.2	57

When submitted to a monoharmonic excitation of constant amplitude F and varying frequency ω, the system's displacement follows a periodic orbit whose amplitude X can be characterized by so-called Frequency Response Curves (FRCs) (Fig. 1). They show that both the cubic and the piecewise linear systems are hardening: the amplitude peak shifts to higher frequencies as the amplitude increases. Furthermore, the shift is such that there can exist multiple responses to the same excitation frequency. Some of the orbits are stable and other are unstable, the latter meaning that the system's displacement will diverge from the orbit towards some other (stable) orbit. Such responses cannot be observed experimentally without external stabilization.

One stabilization method applies feedback control on the displacement. A target in displacement x^* is

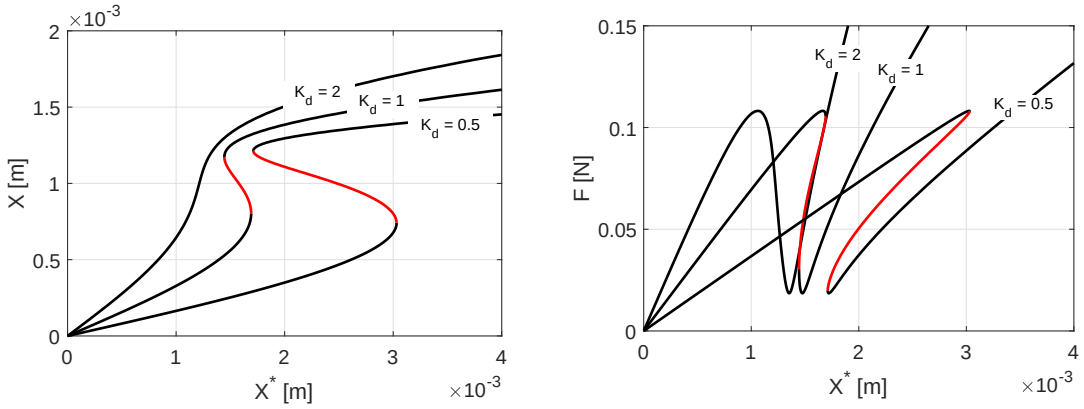

(a) (b)

Figure 2: (a) Displacement amplitude X and (b) excitation amplitude F of the cubic system excited by a differential controller of gain K_d and monoharmonic target of amplitude X^* of constant frequency $\omega = 12$ Hz

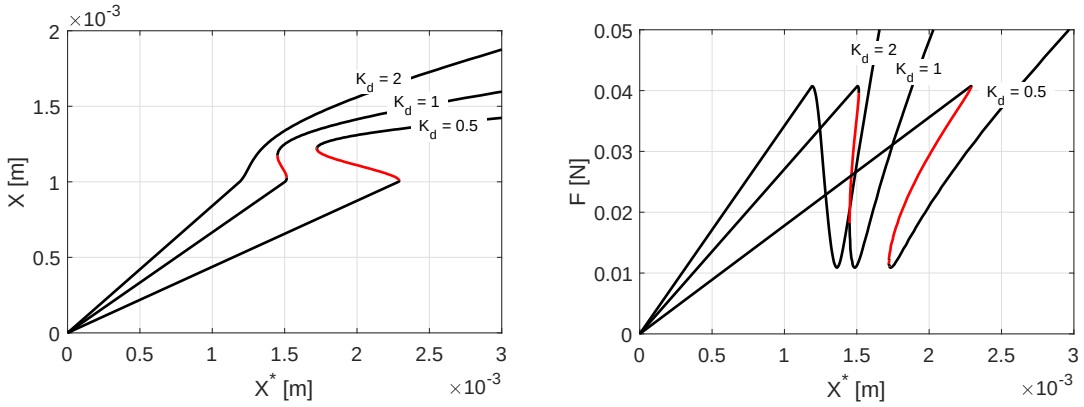

(a) (b)

Figure 3: (a) Displacement amplitude X and (b) excitation amplitude F of the piecewise cubic system excited by a differential controller of gain K_d and monoharmonic target of amplitude X^* of constant frequency $\omega = 7$ Hz

introduced and the excitation signal is generated by a differential controller of gain K_d:

$$f(t) = K_d[\dot{x}^*(t) - \dot{x}(t)]. \tag{4}$$

By combining Eqs. 1 and 4, an equivalent equation of motion can be rewritten:

$$M\ddot{x}(t) + [C + K_d]\dot{x}(t) + Kx(t) + f_{\text{NL}}(x, \dot{x}, t) = K_d\dot{x}^*(t). \tag{5}$$

The effect of the controller on the system's damping is apparent and the excitation is fully defined by the target x^*. When x^* is monoharmonic, both the displacement amplitude X and excitation amplitude F depend on the target amplitude X^*, as shown in Figs. 2 and 3 for a constant excitation frequency ω. The controller gain K_d affects the stability of the periodic orbits and for a high enough value, all the orbits become stable at constant ω. Any orbit of the FRC can therefore be identified experimentally by considering a monoharmonic x^* at frequency ω and tuning the amplitude X^* until reaching the displacement amplitude X of the desired orbit.

3 Control invasiveness

Nonlinear systems respond in general with multiple harmonics. A Fourier decomposition can therefore be made on the displacement signal x to obtain its Fourier coefficients:

$$x(t) = X_0 + \sum_{k=1}^{N_H} X_{ks} \sin(k\omega t) + X_{kc} \cos(k\omega t). \tag{6}$$

In practice, only a limited number of harmonics N_H is considered. Identically, the Fourier coefficients of the target x^* and the excitation f are defined as follows:

$$x^*(t) = X_0^* + \sum_{k=1}^{N_H} X_{ks}^* \sin(k\omega t) + X_{kc}^* \cos(k\omega t), \tag{7}$$

$$f(t) = F_0 + \sum_{k=1}^{N_H} F_{ks} \sin(k\omega t) + F_{kc} \cos(k\omega t). \tag{8}$$

Eq. 4 defines the relation between the Fourier coefficients of every signal $\forall k \in \{1, \dots, N_H\}$:

$$\begin{cases} F_0 = 0 \\ F_{ks} = -kK_d(X_{kc}^* - X_{kc}) \\ F_{kc} = kK_d(X_{ks}^* - X_{ks}). \end{cases} \tag{9}$$

The non-fundamental harmonics ($k \geq 2$) of the displacement x therefore influence the excitation f. As a consequence, the response of the system is different to the one it would have if it were vibrating under a monoharmonic excitation: the controller is invasive. A way to render the controller non-invasive is to cancel every non-fundamental harmonic of f by constraining the target x^*:

$$\begin{cases} X_{ks}^* = X_{ks} \\ X_{kc}^* = X_{kc} \end{cases} \Leftrightarrow \begin{cases} F_{ks} = 0 \\ F_{kc} = 0 \end{cases} \qquad \forall k \in \{2, \dots, N_H\}. \tag{10}$$

There is therefore a need to estimate the Fourier coefficients of x to generate an appropriate target x^*.

4 Adaptive filters

Blasko used adaptive filters to eliminate harmonic noise in a continuous manner — i.e. "online" — without interfering with the stability of feedback control loops [11]. This method can be applied to estimate the Fourier coefficients of the displacement signal x and eliminate unwanted harmonics in the excitation signal f, following Eq. 10. The reader is invited to consult [12] for technical details on adaptive filters. A collection of purely harmonic signals is defined

$$\mathbf{q}(t) = \begin{bmatrix} q_0(t) \\ q_{1s}(t) \\ q_{1c}(t) \\ q_{2s}(t) \\ \vdots \\ q_{N_H c}(t) \end{bmatrix} = \begin{bmatrix} 1 \\ \sin(\omega t) \\ \cos(\omega t) \\ \sin(2\omega t) \\ \vdots \\ \cos(N_H \omega t) \end{bmatrix}. \tag{11}$$

A linear combination of these harmonics signals is made with the weights

$$\mathbf{w}(t) = \begin{bmatrix} w_0(t) \\ w_{1s}(t) \\ w_{1c}(t) \\ w_{2s}(t) \\ \vdots \\ w_{N_H c}(t) \end{bmatrix} \tag{12}$$

to synthesize the output of the controller

$$y(t) = \mathbf{w}^T(t)\mathbf{q}(t). \tag{13}$$

The weights vary through time according to algorithm whose objective is to reduce the error

$$\epsilon(t) = x(t) - y(t) \tag{14}$$

with x still the displacement of the system. There exist several algorithms, the most known being LMS and RLS, both discrete-time algorithms [12].

At time step i, the LMS algorithm updates the weights in a rather simple manner [12]:

$$\mathbf{w}(t_{i+1}) = \mathbf{w}(t_i) + \mu\mathbf{q}(t_i)\epsilon(t_i). \tag{15}$$

The step size coefficient μ is an internal parameter. The sampling frequency f_s has a large effect on the performance of discrete-time filters. Therefore, the coefficient is normalized:

$$\mu' = \mu f_s. \tag{16}$$

The RLS algorithm is more complicated; past time steps have an influence on the weight update through the estimation of the inverse covariance matrix for $\mathbf{q}$, noted $\mathbf{P}$ [12]:

$$\mathbf{k}(t_i) = \frac{\lambda^{-1}\mathbf{P}(t_{i-1})\mathbf{q}(t_i)}{1 + \lambda^{-1}\mathbf{q}^T(t_i)\mathbf{P}(t_{i-1})\mathbf{q}(t_i)}, \tag{17}$$

$$\hat{\epsilon}(t_i) = x(t_i) - \mathbf{w}^T(t_{i-1})\mathbf{q}(t_i), \tag{18}$$

$$\mathbf{w}(t_i) = \mathbf{w}(t_{i-1}) + \mathbf{k}(t_i)\hat{\epsilon}(t_i), \tag{19}$$

$$\mathbf{P}(t_i) = \lambda^{-1}\mathbf{P}(t_{i-1}) - \lambda^{-1}\mathbf{k}(t_i)\mathbf{q}^T(t_i)\mathbf{P}(t_{i-1}). \tag{20}$$

The performance of the filter is governed by the forgetting factor λ, an internal parameter. It can be normalized

$$\lambda = 2^{-N/f_s} \tag{21}$$

where N can be seen as the half-life of the information in time units.

For a successful filtering (i.e. $\epsilon \ll x$ and $\mathbf{w}(t) \approx \mathbf{w}$), the weights are good estimators of the Fourier coefficients (see the parallel between Eqs. 6 and 13):

$$\begin{cases} X_0 \approx w_0 \\ X_{ks} \approx w_{ks} \\ X_{kc} \approx w_{kc} \end{cases} \quad \forall k \in \{1, \ldots, N_H\}. \tag{22}$$

The method to achieve non-invasive feedback stabilization is shown in Fig. 4. There are two loops in parallel: the feedback loop compares the displacement x to the target x^* in order to generate the excitation f through a differential controller, and the filter loop estimates the Fourier coefficients of x through an adaptive filter

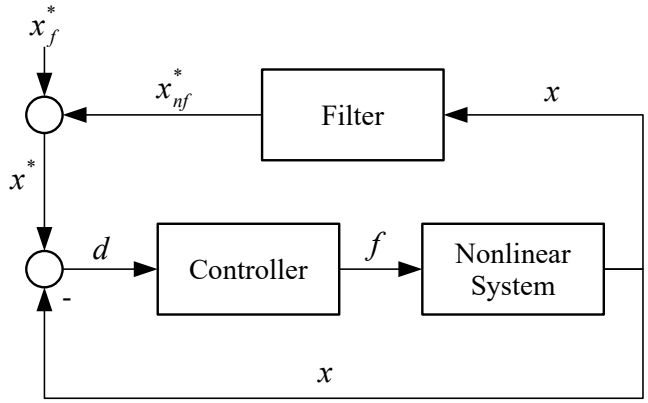

Figure 4: Feedback and filter loops used to achieve non-invasive feedback stabilization of the system's periodic orbits

generating the non-fundamental part of the target following Eq. 10:

$$x_{nf}^*(t) = \sum_{k=2}^{N_H} X_{ks}^* \sin(k\omega t) + X_{kc}^* \cos(k\omega t). \tag{23}$$

The fundamental part x_f^* of the target is a monoharmonic signal of frequency ω and amplitude X^* tuned by the user to identify the periodic orbit of same frequency and desired amplitude X.

5 Parameter Study

The performance of the method is evaluated for canceling the controller invasiveness. It is influenced by the number of harmonics N_H considered by the adaptive filter and the algorithm used. The latter possesses internal parameters as well.

A third nonlinear system is introduced, possessing a non-smooth friction law:

$$f_{\text{NL},3}(x, \dot{x}, t) = \begin{cases} -0.05 & \text{for } \dot{x} < 0 \text{ mm} \\ 0 & \text{for } \dot{x} = 0 \text{ mm} \\ 0.05 & \text{for } \dot{x} > 0 \text{ mm}, \end{cases} \tag{24}$$

called the friction system. It does not possess unstable orbits like the cubic or the piecewise linear system do. Stabilization is therefore useless in this particular case, but assessing the performance of the method on a non-smooth friction nonlinearity is relevant.

For this study, the cubic and piecewise linear systems are stabilized on an unstable orbit and the friction system on a similar orbit. The orbits are characterized in Table 2.

Table 2: Characteristics of the orbits identified in Section 5 (unstable for the cubic and piecewise linear systems) and parameters of the feedback stabilization

System	ω [Hz]	X [mm]	F [N]	X^* [mm]	K_d [Ns/m]
Cubic	12	1.17	0.03	1.19	5
Piecewise linear	7	1.11	0.03	1.13	5
Friction	7	1.23	0.1	1.60	5

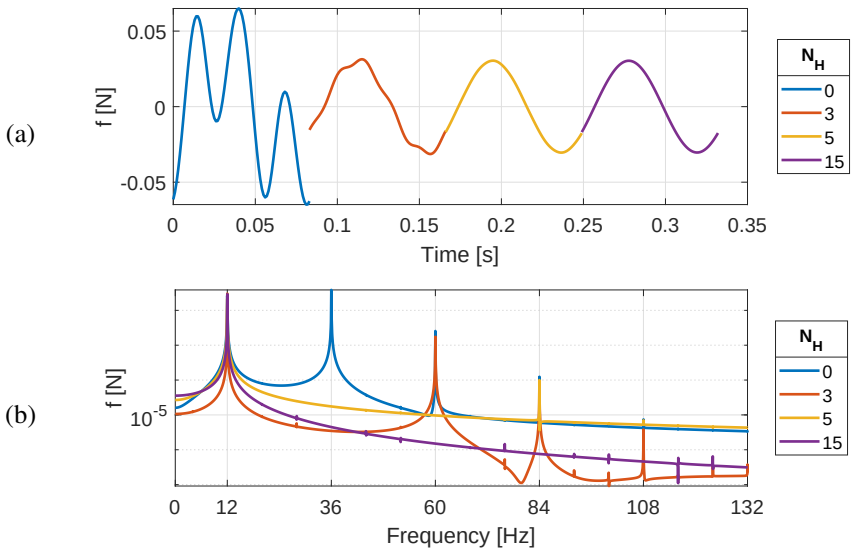

Figure 5: Excitation signal in (a) time and (b) frequency of the cubic system depending on the number N_H of harmonics considered in the adaptive filter

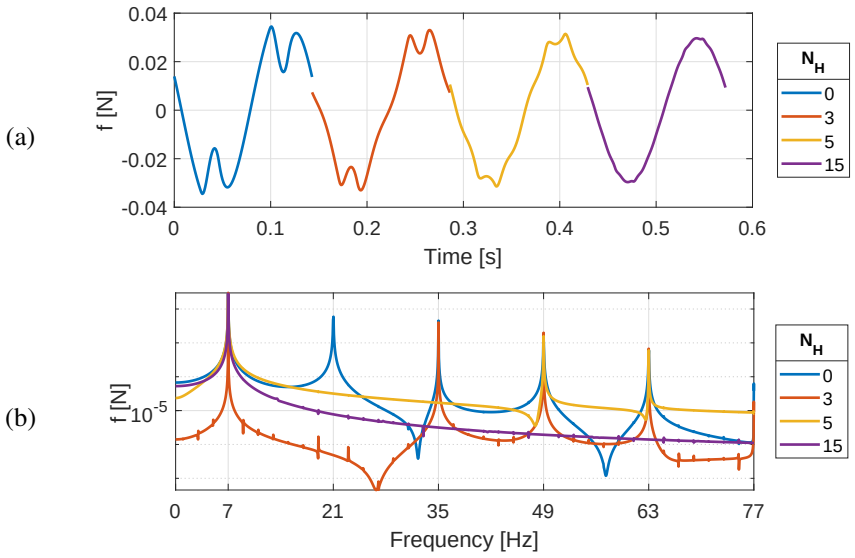

Figure 6: Excitation signal in (a) time and (b) frequency of the piecewise linear system depending on the number N_H of harmonics considered in the adaptive filter

5.1 Number of harmonics

The performance of the adaptive filtering is linked to the number of harmonics N_H considered in the adaptive filter. The present method cancels invasiveness of the harmonics for which Eq. 10 is met. Non-fundamental harmonics generated by the nonlinearities of the system must be taken into account for the stabilization to be non-invasive at this frequency.

The three systems are stabilized on the orbit characterized in Table 2 with various numbers of harmonics N_H being considered in the adaptive filter. After having reached steady-state, one period of the excitation signal is shown in Figs. 5a to 7a. The spectrum of the signal is shown in Figs. 5b to 7b. The fully invasive case (i.e. for a monoharmonic $x^* = x_f^*$ and without an adaptive filter) is shown with $N_H = 0$.

Once the Fourier coefficients of a harmonic are estimated by the filter, the harmonic is reduced to insignificant levels in the excitation signal. The cubic system exhibits a very strong third and a slight fifth harmonics while

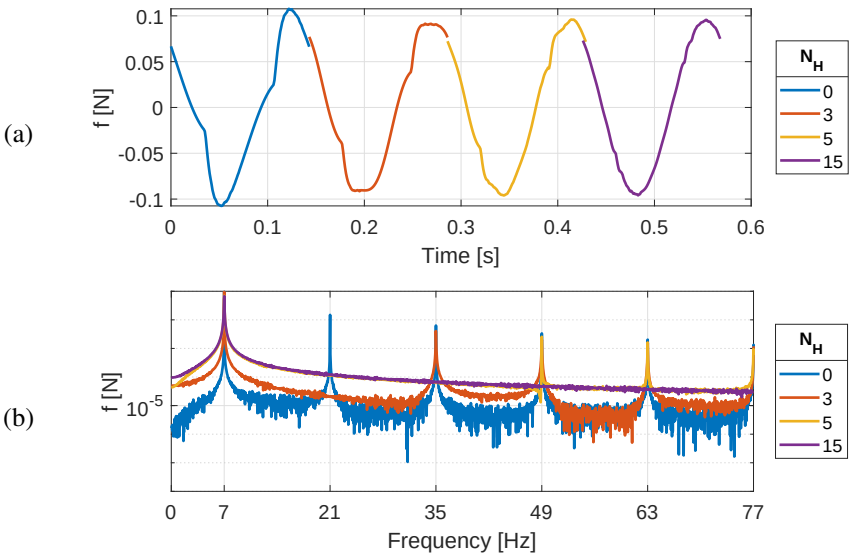

Figure 7: Excitation signal in (a) time and (b) frequency of the friction system depending on the number N_H of harmonics considered in the adaptive filter

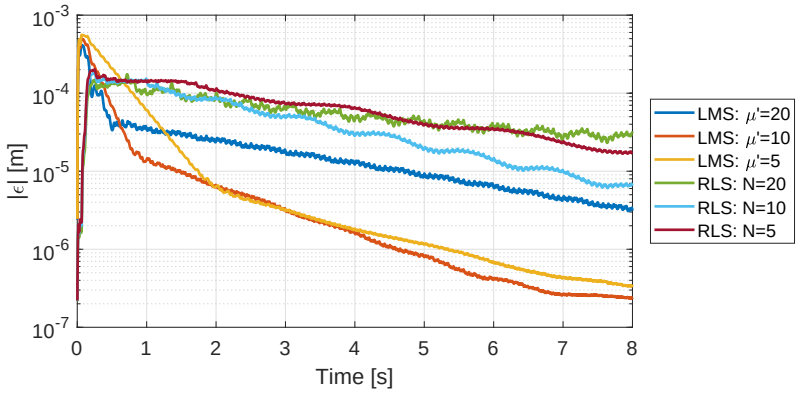

Figure 8: Evolution of the absolute error ϵ between x and y for various adaptive filter algorithms and parameters on the piecewise linear system (ϵ smoothed over $1/\omega = 1/7$ s)

the higher ones are not significant. Unsurprisingly, the non-smooth systems exhibit a much richer harmonic content with harmonics up to 7 reaching significant amplitudes. The harmonics considered by the adaptive filter are however successfully canceled.

5.2 Algorithm

The effect of the internal parameter of the LMS algorithm μ' (see Eq. 16) is shown in Fig. 8. Larger values increase the correction step size and render the filter more reactive. However, the magnitude of ϵ converges to higher values. Smaller values of μ' make the weights converge more slowly but ϵ is expected to eventually reach a lower magnitude. However, the filter being in a feedback loop prevents this. A value of $\mu' = 10$ seems a good compromise in this case, leading to convergence after less than a second.

The effect of the internal parameter of the RLS algorithm N (see Eq. 21) is shown in Fig. 8 as well. The larger λ is, the more important past time steps are. It seems that the RLS algorithm is less efficient than the simpler LMS algorithm in this context.

6 Conclusion

Feedback stabilization by differential control is a simple and effective way to experimentally identify unstable orbits of a nonlinear system. However, non-fundamental harmonics in the displacement signal generated by the nonlinearities in the system affect the excitation signal. Consequently, the orbits identified are different to the ones that the system would have if it were excited by a monoharmonic excitation signal. This invasiveness can be avoided by constraining the control target such that it cancels the non-fundamental harmonics of the controller's input, rendering the excitation signal monoharmonic.

The constraint consists in imposing that the target's non-fundamental harmonics equal the ones of the displacement. This paper presents a method to achieve this online — i.e. continuously in time — by using adaptive filters. Harmonic signals are combined to synthesize a signal identical to the displacement signal. The weights of this combination are good estimators of the Fourier coefficients.

Harmonics can be selectively removed from the excitation signal until it is monoharmonic. The feedback stabilization is not lost and the controller becomes non-invasive. The performance of such a method is shown for three systems: one containing a smooth nonlinear stiffness, one containing a non-smooth nonlinear stiffness, and one containing a non-smooth nonlinear damping. Two algorithms used in the adaptive filter are compared and their internal parameters studied to find a compromise between a small filtering error and a fast convergence.

Acknowledgements

G. Abeloos wishes to express his gratitude toward the F.R.S./FNRS for funding this research through the FRIA grant.

References

[1] K. Pyragas, "Continuous control of chaos by self-controlling feedback," *Physics Letters A*, vol. 170, no. 6, pp. 421–428, 1992. [Online]. Available: https://doi.org/10.1016/0375-9601(92)90745-8

[2] J. Sieber and B. Krauskopf, "Control-based continuation of periodic orbits with a time-delayed difference scheme," *International Journal of Bifurcation and Chaos*, vol. 17, no. 8, pp. 2576–2593, 2007. [Online]. Available: https://doi.org/10.1142/S0218127407018646

[3] J. Sieber and B. Krauskopf, "Control based bifurcation analysis for experiments," *Nonlinear Dynamics*, vol. 51, pp. 356–377, 2008. [Online]. Available: https://doi.org/10.1007/s11071-007-9217-2

[4] J. Sieber, A. Gonzalez-Buelga, S. A. Neild, D. J. Wagg, and B. Krauskopf, "Experimental continuation of periodic orbits through a fold," *Physical Review Letters*, vol. 100, no. 24, p. 244101, 2008. [Online]. Available: https://link.aps.org/doi/10.1103/PhysRevLett.100.244101

[5] D. A. Barton and S. G. Burrow, "Numerical continuation in a physical experiment: Investigation of a nonlinear energy harvester," *Journal of Computational and Nonlinear Dynamics*, vol. 6, no. 1, p. 011010, 2011. [Online]. Available: https://doi.org/10.1115/DETC2009-87318

[6] D. A. Barton and J. Sieber, "Systematic experimental exploration of bifurcations with noninvasive control," *Physical Review E*, vol. 87, p. 052916, 2013. [Online]. Available: https://link.aps.org/doi/10.1103/PhysRevE.87.052916

[7] L. Renson, A. Gonzalez-Buelga, D. A. Barton, and S. A. Neild, "Robust identification of backbone curves using control-based continuation," *Journal of Sound and Vibration*, vol. 367, pp. 145–158, 2016. [Online]. Available: https://doi.org/10.1016/j.jsv.2015.12.035

[8] D. A. Barton, "Control-based continuation: Bifurcation and stability analysis for physical experiments," *Mechanical Systems and Signal Processing*, vol. 84, no. B, pp. 54–64, 2017. [Online]. Available: http://dx.doi.org/10.1016/j.ymssp.2015.12.039

[9] L. Renson, D. A. Barton, and S. A. Neild, "Experimental tracking of limit-point bifurcations and backbone curves using control-based continuation," *International Journal of Bifurcation and Chaos*, vol. 27, no. 1, p. 1730002, 2017. [Online]. Available: https://doi.org/10.1142/S0218127417300026

[10] L. Renson, A. D. Shaw, D. A. Barton, and S. A. Neild, "Application of control-based continuation to a nonlinear structure with harmonically coupled modes," *Mechanical Systems and Signal Processing*, vol. 120, pp. 449–464, 2019. [Online]. Available: https://doi.org/10.1016/j.ymssp.2018.10.008

[11] V. Blasko, "A novel method for selective harmonic elimination in power electronic equipment," *IEEE Transactions on Power Electronics*, vol. 22, no. 1, pp. 223–228, 2007. [Online]. Available: https://doi.org/10.1109/TPEL.2006.886599

[12] S. Haykin, *Adaptive filter theory*, 3rd ed. New Jersey: Prentice Hall, 1996.